NATIONAL ADVISORY COMMITTEE FOR AERONAUTICS

TECHNICAL NOTE 2875

BEHAVIOR IN PURE BENDING OF A LONG MONOCOQUE BEAM OF CIRCULAR-ARC CROSS SECTION

By Robert W. Fralich, J. Mayers, and Eric Reissner

Langley Aeronautical Laboratory
Langley Field, Va.

Washington
January 1953

NATIONAL ADVISORY COMMITTEE FOR AERONAUTICS

TECHNICAL NOTE 2875

BEHAVIOR IN PURE BENDING OF A LONG MONOCOQUE BEAM OF CIRCULAR-ARC CROSS SECTION

By Robert W. Fralich, J. Mayers, and Eric Reissner

SUMMARY

An analysis is made of the behavior under a loading of pure bending moment of a thin, infinitely long, pure-monocoque beam having a constant, doubly symmetric, circular-arc cross section. Bending moments, deflections, and stresses are obtained. The analysis shows a nonlinear behavior in bending which leads ultimately to a maximum moment and instability.

INTRODUCTION

The pure-monocoque beam, with no internal bulkheads, ribs, spars, or stiffeners, represents a limiting structure which designers can approach in an attempt to obtain thin hollow wings with low fabrication and assembly costs. Examination of the structural behavior of the pure-monocoque beam is, therefore, of interest in order to determine its favorable or unfavorable characteristics. In particular, an understanding of the nature and growth of the cross-sectional distortion that arises from the tendency for the beam to flatten under longitudinal bending loads is important. With sufficient flattening, the beam bending stiffness can be reduced to a point at which the beam no longer will sustain an increase in bending moment, and instability results. The related problem in connection with circular cylinders is well-known and has been discussed by Brazier (ref. 1).

In the present paper a thin, infinitely long, pure-monocoque beam having a constant, doubly symmetric, circular-arc cross section is analyzed under a loading of pure bending moment (fig. 1). This loading produces identical deformation of all cross sections and, therefore, permits a relatively simple structural analysis to be made. Elastic behavior is assumed and local buckling is not considered.

In an actual pure-monocoque circular-arc wing, these idealized conditions of structure and loading would not be realized - the cross section and bending moment would vary spanwise and the bending moments

would be produced by lateral forces applied directly to the wing surface. At least the order of magnitude of the distortion of any cross section in the actual wing (away from the root or tip bulkheads) could probably be determined, however, by assuming the cross section to be part of an infinitely long uniform beam subjected to a uniform bending moment equal to the actual local bending moment.

An analysis of the idealized structure is given in the appendix. The body of the paper contains the results of the analysis and describes the distortion characteristics and stresses of the pure-monocoque beam under uniform bending moment.

Part of the work presented herein was carried out in June 1951 while the last-named author was temporarily at the Langley Laboratory, and it was continued by correspondence.

SYMBOLS

A, B, C	constants
b	semiwidth of cover plates, in.
D	flexural stiffness of cover plates, $\frac{Et^3}{12(1 - \mu^2)}$, in-lb
E	Young's modulus for beam material, lb/in.^{2}
h	rise of circular arc measured from undeformed middle surface of beam to middle surface of covers, in.
I_0	moment of inertia of undeformed beam cross section, in.^{4}
k	curvature of beam axis, in.$^{-1}$
M_x, M_y	plate bending moments on cross sections perpendicular to x- and y-axes, respectively, in-lb/in.
m	total beam bending moment, in-lb
N_x, N_y	plate middle-surface forces in x- and y-directions, lb/in.
Q_y	plate shearing force in xz-plane, lb/in.

r	radius of curvature of circular-arc cross section, in.
t	thickness of cover plate, in.
W	radial deflection of point in middle surface of cover of bent beam, in.
w	total radial deflection of point in middle surface of cover plate, in.
x, y, z	coordinates
γ	parameter, $\gamma = \lambda b$
ϵ_x	plate axial strain
ϵ_{x_o}	strain at surface passing through beam edges
λ	parameter defined by $4\lambda^4 = \frac{Etk^2}{D}$, in.$^{-1}$
μ	Poisson's ratio for beam material, $\mu = 0.316$ for all computations
$\sigma_{x_{cr}}$	local buckling stress of compression cover
φ, Φ	stress functions
∇^4	linear differential operator defined by $\frac{\partial^4}{\partial x^4} + 2\frac{\partial^4}{\partial x^2 \partial y^2} + \frac{\partial^4}{\partial y^4}$

Subscripts:

b	bottom or tension cover
t	top or compression cover

RESULTS

Relationship of Bending Moment and Beam Curvature

For calculations of the over-all stiffness of a beam, a knowledge of the relationship between bending moment and longitudinal beam curvature is important. This relationship for the pure-monocoque beam is shown nondimensionally in figure 2.

Unlike solid beams or shell beams with internal stiffening, which have linear moment-curvature relationships, the pure-monocoque beam exhibits a nonlinear relationship. This nonlinear behavior is a consequence of the continual reduction in cross-sectional moment of inertia as bending progresses. This reduction in moment of inertia or resistance to bending leads ultimately to a maximum moment. The slight spread in the vicinity of the maximum among the curves for different values of t/h is a result of taking into account the shift in the neutral surface of the beam due to the unsymmetric behavior of the top and bottom covers. If this small effect is neglected, the maximum value of the bending moment is $m = 0.285 \frac{EtI_0}{rh}$, corresponding to a nominal midchord critical stress of $0.285 \frac{Et}{r}$ based on the geometry of the undeformed cross section, or a midchord critical stress of $0.36 \frac{Et}{r}$ based on the geometry of the flattened configuration. This maximum value of bending moment which occurs at a beam curvature of $k = 0.52 \frac{t}{rh}$ may be considered to be the upper limit of the strength of the beam.

Distortion of Cross Section

A measure of the cross-sectional distortion is given by the magnitude of the beam-thickness change at midchord. The ratio of midchord beam thickness of the deformed cross section $h_t(0) + h_b(0)$ to midchord beam thickness of the undeformed cross section $2h$ is plotted in figure 3 as a function of the beam-curvature parameter. From the figure, the flattening is seen to be appreciable over most of the loading range, and at the value of the beam-curvature parameter corresponding to the maximum bending moment, flattening has reduced the original beam thickness by almost 30 percent. The effect of different t/h ratios does not appear in this plot since the thickness change is independent of neutral-surface shift.

The cover deflections at every chordwise point may also be of interest. These deflections can be computed from equations (48) and (49) or equation (65) in the appendix. A typical chordwise plot of the cover deflections, in which the small effect of the neutral-surface shift is neglected, is shown in figure 4 for a beam loaded very nearly to its maximum moment.

Stresses

The magnitudes of the axial stresses in the beam are best indicated by the magnitudes of the axial stresses at the midchord where they have their greatest values (at least up to maximum moment). For each cover, the ratio of midchord axial stress to the linear-theory stress at the same beam curvature is plotted in figure 5 as a function of the nondimensional beam-curvature parameter for values of t/h equal to 0 and 0.4. When compared at equal beam curvatures, the stresses of the present theory are always of less magnitude as a consequence of the flattening.

The ratio of midchord axial stress for each cover (with the small effect of neutral-surface shift neglected) to the linear-theory stress at the same bending moment is plotted in figure 6 as a function of the nondimensional bending-moment parameter. The result indicates that, at the same value of bending moment, the cover stress in the present theory is greater than the linear-theory stress. This condition is a result of flattening decreasing the moment of inertia more rapidly than it decreases the beam thickness.

DISCUSSION

The results indicate a nonlinear relationship between bending moment and beam curvature that arises from the low chordwise bending stiffness of the covers and ultimately leads to an instability. The results also indicate that, in general, an appreciable profile flexibility exists which may be detrimental from an aerodynamic point of view. In order for completely hollow wings to resist large distortions, additional chordwise bending stiffness must be realized in the covers (e.g., by integrally stiffened or sandwich construction).

In the analysis the effect of chordwise middle-surface stresses on the deflections is neglected. Order-of-magnitude considerations indicate that such an assumption is justified for cross sections where $(b/r)^2$ and $(t/h)^2$ are small compared with unity. These conditions are satisfied, in general, for shallow sections such as would be considered for thin wings.

The effect of local buckling of the compression cover has been omitted from the analysis. Its importance with respect to the present problem can, however, be estimated in the following manner:

The theoretical buckling stress in uniform compression of a long curved plate is given by the relation

$$\sigma_{x_{cr}} = 0.6 \frac{Et}{r}$$

which applies to both simply supported and clamped long plates if the curvature parameter $\frac{4b^2}{rt}\sqrt{1 - \mu^2}$ is greater than about 60. In this range more than one buckle appears in the circumferential direction and the buckling stress becomes practically independent of edge conditions. It is well-known, however, that the "classical" stress of $0.6 \frac{Et}{r}$ is never attained in actual curved plates and requires modification by an appropriate "knockdown" factor. This factor is a function of the ratio of radius to plate thickness and has been discussed in many papers, for example, reference 2. In this reference the buckling stress is given by the empirical relation

$$\sigma_{x_{cr}} = \left(0.588 - 0.000433 \frac{r}{t}\right) \frac{Et}{r}$$

for plates having radius-thickness ratios between 500 and 1,000. The knockdown factor in the region $r/t > 1{,}000$ can be taken as the same or less than that at $\frac{r}{t} = 1{,}000$.

Local buckling of the compression cover in bending is estimated to occur if the stress measured at the midchord is between 20 and 40 percent higher than the stress required for local buckling in uniform compression. The estimates are based on curved-plate linear-theory considerations and experimental results for cylinders (ref. 3). If an average value of 1.3 is assumed for the ratio of the critical stresses, the stress for local buckling in bending becomes

$$\sigma_{x_{cr}} = \left(0.765 - 0.000563 \frac{r}{t}\right) \frac{Et}{r}$$

Since the midchord stress corresponding to flattening instability is approximately $0.36\frac{Et}{r}$ (see fig. 5), local buckling of the compression cover would be expected to occur after flattening instability for $r/t < 720$ and to precede flattening instability for $r/t > 720$. By taking flattening into account, however, this value of r/t is decreased, since the chordwise curvature of the covers, and hence, the critical compressive stress, is decreased.

CONCLUDING REMARKS

An analysis is made of the behavior under a loading of pure bending moment of a thin, infinitely long, pure-monocoque beam having a constant, doubly symmetric, circular-arc cross section. Bending moments, deflections, and stresses are obtained. The analysis shows a nonlinear relationship between bending moment and beam curvature that leads ultimately to a maximum moment and instability. If no interaction is assumed between local buckling of the compression cover and flattening instability, local buckling should precede flattening instability of the beam when the radius-thickness ratio of the covers is greater than about 720 and flattening instability should precede local buckling when this ratio is smaller than about 720.

Langley Aeronautical Laboratory,
National Advisory Committee for Aeronautics,
Langley Field, Va., October 16, 1952.

APPENDIX

ANALYSIS OF IDEALIZED STRUCTURE UNDER LOADING OF PURE BENDING MOMENT

Statement of Problem and Assumptions

The behavior of the idealized structure under a loading of uniform bending moment can be determined from consideration of the equilibrium conditions for a small element in a chordwise strip in each of the covers of the bent beam (see fig. 7). A reduction of the problem to the analysis of a chordwise strip is justified on the basis of symmetry considerations, since all chordwise sections behave identically under the given loading conditions. The small elements and the resultant forces and moments acting upon them, together with the sign convention used, are shown in figure 7. The circumferential middle-surface forces N_{y_t} and N_{y_b} are not included in the analysis since order-of-magnitude calculations indicate that, for shallow cross sections, the effect of the circumferential forces on the deflections are not of first-order importance.

The relative simplicity of the following analysis and the resulting explicit formulas, in contrast with Brazier's work on the circular cylindrical shell, are due to the fact that the shell sections considered are shallow. The present analysis may be readily extended to other than circular-arc sections by retaining the shallow-section assumption.

Derivation of Basic Equations

Since all chordwise sections behave identically under the given loading condition, only force equilibrium in the z-direction and moment equilibrium about the x-axis have to be considered. For a small element in a chordwise strip of the top or compression cover, these equilibrium conditions are

$$\frac{dQ_{y_t}}{dy} - N_{x_t}k = 0 \qquad (1)$$

and

$$\frac{dM_{y_t}}{dy} - Q_{y_t} = 0 \tag{2}$$

where $-k$ is the beam curvature, which is constant along the length of the beam. For a small element in a chordwise strip of the bottom or tension cover, the equilibrium conditions are

$$\frac{dQ_{y_b}}{dy} - N_{x_b}k = 0 \tag{3}$$

and

$$\frac{dM_{y_b}}{dy} - Q_{y_b} = 0 \tag{4}$$

Elimination of Q_{y_t} and Q_{y_b} from each of the pairs of equations yields

$$\frac{d^2M_{y_t}}{dy^2} - N_{x_t}k = 0 \tag{5}$$

and

$$\frac{d^2M_{y_b}}{dy^2} - N_{x_b}k = 0 \tag{6}$$

Since all chordwise sections behave identically, the cross-sectional distortion is independent of the axial coordinate x. As a result, for each of the chordwise strips, the moment-distortion relationships from plate theory become

$$M_{y_t} = -D\left[\frac{d^2W_t(y)}{dy^2} - \mu k\right] \tag{7}$$

and

$$M_{y_b} = -D\left[\frac{d^2W_b(y)}{dy^2} - \mu k\right] \tag{8}$$

where the radial deflections $W_t(y)$ and $W_b(y)$ are positive when directed downward in figure 7. Substitution of these relations for M_{y_t} and M_{y_b} into the two equilibrium equations (5) and (6) yields

$$-D\frac{d^4W_t(y)}{dy^4} - N_{x_t}k = 0 \tag{9}$$

and

$$-D\frac{d^4W_b(y)}{dy^4} - N_{x_b}k = 0 \tag{10}$$

The axial forces N_{x_t} and N_{x_b} can be written in terms of the axial strains as

$$N_{x_t} = Et\epsilon_{x_t} \tag{11}$$

and

$$N_{x_b} = Et\epsilon_{x_b} \tag{12}$$

The strains, measured from the as yet undetermined neutral surface of the cross section, are

$$\epsilon_{x_t} = -kh\left(1 - \frac{y^2}{b^2}\right) - \epsilon_{x_o} + kW_t(y) \tag{13}$$

and

$$\epsilon_{x_b} = kh\left(1 - \frac{y^2}{b^2}\right) - \epsilon_{x_o} + kW_b(y) \tag{14}$$

where ϵ_{x_o} is the strain at the surface passing through the beam edges and $h\left(1 - \frac{y^2}{b^2}\right)$ is the distance from this surface to the middle surface of the undeformed covers. The latter quantity gives the rise at any point y in good approximation for shallow sections. With the foregoing relations, the equilibrium equations (9) and (10) become

$$-D\frac{d^4W_t(y)}{dy^4} + Etk\left[kh\left(1 - \frac{y^2}{b^2}\right) + \epsilon_{x_o} - kW_t(y)\right] = 0 \tag{15}$$

and

$$-D\frac{d^4W_b(y)}{dy^4} - Etk\left[kh\left(1 - \frac{y^2}{b^2}\right) - \epsilon_{x_o} + kW_b(y)\right] = 0 \tag{16}$$

Rearranging the terms gives

$$D\frac{d^4W_t(y)}{dy^4} + Etk^2W_t(y) = Etk^2h\left(1 - \frac{y^2}{b^2}\right) + Etk\epsilon_{x_o} \tag{17}$$

and

$$D\frac{d^4W_b(y)}{dy^4} + Etk^2W_b(y) = -Etk^2h\left(1 - \frac{y^2}{b^2}\right) + Etk\epsilon_{x_o} \tag{18}$$

The two foregoing equations are the differential equations of equilibrium for the chordwise strips in each of the covers. Each equation may be noted to be that of a beam of unit width on an elastic foundation, where the left-hand side of each equation represents the restoring

forces due to the cover bending stiffness and the elastic foundation and the right-hand side represents the forces causing deflection.

The deflections can be obtained from the equilibrium equations for a given set of boundary conditions, which in this problem are taken to be

$$W_t(\pm b) = W_b(\pm b) = 0$$

$$\frac{dW_t(\pm b)}{dy} = \frac{dW_b(\pm b)}{dy}$$

and

$$-2\mu k + \frac{d^2W_t(\pm b)}{dy^2} + \frac{d^2W_b(\pm b)}{dy^2} = 0$$

These conditions indicate that no edge deflections exist relative to the bent beam, that the edge angles are maintained between the two covers, and that no resultant edge moments are permitted. The last condition is obtained from $M_{y_t}(\pm b) + M_{y_b}(\pm b) = 0$ by virtue of the moment-distortion relationships.

Before the deflections can be completely defined, the strain at the surface passing through the beam edges is required. Because of symmetry, no resultant axial force exists in the beam at any cross section. This condition is given by the relation

$$\int_{-b}^{b} N_{x_t}\, dy + \int_{-b}^{b} N_{x_b}\, dy = 0 \tag{19}$$

and leads to the relation for the strain at the surface passing through the beam edges

$$\epsilon_{x_o} = \frac{k}{4b}\int_{-b}^{b} \left[W_t(y) + W_b(y)\right] dy \tag{20}$$

when the force-strain relations are substituted into equation (19).

Alternate Derivation of Basic Equations

The basic differential equations can be derived by considering the total deflection of small elements in chordwise strips of each of the covers measured from the initially nonstressed position of the elements. Since the deflections measured in this manner will be large compared with the cover thicknesses, the equilibrium conditions for the small elements must be expressed by the equations of large-deflection theory of shallow cylindrical shells (ref. 4).

For the top cover, these equations are

$$\frac{1}{E}\nabla^4\varphi_t(x,y) = \left[\frac{\partial^2 w_t(x,y)}{\partial x\,\partial y}\right]^2 - \frac{\partial^2 w_t(x,y)}{\partial x^2}\left[\frac{\partial^2 w_t(x,y)}{\partial y^2} + \frac{1}{r}\right] \tag{21}$$

and

$$D\nabla^4 w_t(x,y) = t\frac{\partial^2\varphi_t(x,y)}{\partial y^2}\frac{\partial^2 w_t(x,y)}{\partial x^2} + t\frac{\partial^2\varphi_t(x,y)}{\partial x^2}\left[\frac{\partial^2 w_t(x,y)}{\partial y^2} + \frac{1}{r}\right] - 2t\frac{\partial^2\varphi_t(x,y)}{\partial x\,\partial y}\frac{\partial^2 w_t(x,y)}{\partial x\,\partial y} \tag{22}$$

and for the bottom cover, the equations are

$$\frac{1}{E}\nabla^4\varphi_b(x,y) = \left[\frac{\partial^2 w_b(x,y)}{\partial x\,\partial y}\right]^2 - \frac{\partial^2 w_b(x,y)}{\partial x^2}\left[\frac{\partial^2 w_b(x,y)}{\partial y^2} - \frac{1}{r}\right] \tag{23}$$

and

$$D\nabla^4 w_b(x,y) = t\frac{\partial^2\varphi_b(x,y)}{\partial y^2}\frac{\partial^2 w_b(x,y)}{\partial x^2} + t\frac{\partial^2\varphi_b(x,y)}{\partial x^2}\left[\frac{\partial^2 w_b(x,y)}{\partial y^2} - \frac{1}{r}\right] - 2t\frac{\partial^2\varphi_b(x,y)}{\partial x\,\partial y}\frac{\partial^2 w_b(x,y)}{\partial x\,\partial y} \tag{24}$$

where $w_t(x,y)$ and $w_b(x,y)$ are the total deflections and $\varphi_t(x,y)$ and $\varphi_b(x,y)$ are the respective stress functions of the covers. The relationships between the stress functions and the middle-surface forces in the covers are

$$\left.\begin{aligned} \frac{\partial^2\varphi_t(x,y)}{\partial x^2} &= \frac{N_{y_t}}{t} \qquad \frac{\partial^2\varphi_t(x,y)}{\partial y^2} = \frac{N_{x_t}}{t} \qquad \frac{\partial^2\varphi_t(x,y)}{\partial x\,\partial y} = -\frac{N_{xy_t}}{t} \\ \frac{\partial^2\varphi_b(x,y)}{\partial x^2} &= \frac{N_{y_b}}{t} \qquad \frac{\partial^2\varphi_b(x,y)}{\partial y^2} = \frac{N_{x_b}}{t} \qquad \frac{\partial^2\varphi_b(x,y)}{\partial x\,\partial y} = -\frac{N_{xy_b}}{t} \end{aligned}\right\} \quad (25)$$

These equations together with the boundary conditions determine $w_t(x,y)$, $w_b(x,y)$, $\varphi_t(x,y)$, and $\varphi_b(x,y)$. If use is made of the identical behavior of each cross section, the deflections of the elements may be assumed to be

$$w_t(x,y) = -\frac{1}{2}kx^2 + W_t(y) \quad (26)$$

and

$$w_b(x,y) = -\frac{1}{2}kx^2 + W_b(y) \quad (27)$$

where $-\frac{1}{2}kx^2$ is the parabolic deflection of the beam edges due to the uniform bending moment and $W_t(y)$ and $W_b(y)$ are the chordwise deformations of the covers. Since the circumferential forces N_{y_t} and N_{y_b} are not included in the analysis, the stress functions may be taken to be

$$\varphi_t(x,y) = \Phi_t(y) \quad (28)$$

and

$$\varphi_b(x,y) = \Phi_b(y) \quad (29)$$

Substitution of the relations for the deflections and the stress functions into the large-deflection equations gives

$$\frac{1}{E}\frac{d^4\Phi_t(y)}{dy^4} = k\left[\frac{d^2W_t(y)}{dy^2} + \frac{1}{r}\right] \tag{30}$$

$$D\frac{d^4W_t(y)}{dy^4} = -tk\frac{d^2\Phi_t(y)}{dy^2} \tag{31}$$

and

$$\frac{1}{E}\frac{d^4\Phi_b(y)}{dy^4} = k\left[\frac{d^2W_b(y)}{dy^2} - \frac{1}{r}\right] \tag{32}$$

$$D\frac{d^4W_b(y)}{dy^4} = -tk\frac{d^2\Phi_b(y)}{dy^2} \tag{33}$$

After the first equation in each case is integrated twice, the result is

$$\frac{1}{E}\frac{d^2\Phi_t(y)}{dy^2} = k\left[W_t(y) + \frac{y^2}{2r}\right] + C_1y + C_2 \tag{34}$$

and

$$\frac{1}{E}\frac{d^2\Phi_b(y)}{dy^2} = k\left[W_b(y) - \frac{y^2}{2r}\right] + C_3y + C_4 \tag{35}$$

From symmetry considerations, $C_1 = C_3 = 0$ so that substitution of these expressions for $\frac{d^2\Phi_t(y)}{dy^2}$ and $\frac{d^2\Phi_b(y)}{dy^2}$ into the remaining two equations gives

$$D\frac{d^4W_t(y)}{dy^4} + Etk^2W_t(y) = -\frac{Etk^2y^2}{2r} - EtkC_2 \tag{36}$$

and

$$D\frac{d^4W_b(y)}{dy^4} + Etk^2W_b(y) = \frac{Etk^2y^2}{2r} - EtkC_4 \tag{37}$$

The boundary conditions on the total deflections $w_t(x,y)$ and $w_b(x,y)$ are

$$w_t(x,\pm b) = w_b(x,\pm b) = -\frac{1}{2}kx^2$$

$$\frac{\partial w_t(x,\pm b)}{\partial y} = \frac{\partial w_b(x,\pm b)}{\partial y}$$

and

$$M_{y_t}(x,\pm b) + M_{y_b}(x,\pm b) = 0$$

so that the corresponding boundary conditions on $W_t(y)$ and $W_b(y)$ become

$$W_t(\pm b) = W_b(\pm b) = 0$$

$$\frac{dW_t(\pm b)}{dy} = \frac{dW_b(\pm b)}{dy}$$

and

$$-2\mu k + \frac{d^2W_t(\pm b)}{dy^2} + \frac{d^2W_b(\pm b)}{dy^2} = 0$$

The conditions necessary for determining C_2 and C_4 are

$$N_{x_t}(\pm b) = N_{x_b}(\pm b) \tag{38}$$

and

$$\int_{-b}^{b} N_{x_t}\, dy + \int_{-b}^{b} N_{x_b}\, dy = 0 \tag{39}$$

which account for continuity of axial forces at the edges and zero resultant axial thrust. If, in these equations, N_{x_t} and N_{x_b} are written in terms of deflections by use of the relationships between axial forces and stress functions and between stress functions and deflections, the following equations are obtained:

$$\frac{kb^2}{r} + C_2 - C_4 = 0 \tag{40}$$

and

$$k\int_{-b}^{b} \left[W_t(y) + W_b(y)\right] dy + 2b\left(C_2 + C_4\right) = 0 \tag{41}$$

The simultaneous solution of these equations for C_2 and C_4 yields

$$C_2 = -kh - \frac{k}{4b}\int_{-b}^{b} \left[W_t(y) + W_b(y)\right] dy \tag{42}$$

and

$$C_4 = kh - \frac{k}{4b}\int_{-b}^{b} \left[W_t(y) + W_b(y)\right] dy \tag{43}$$

where

$$h = \frac{b^2}{2r}$$

Substitution of these expressions for C_2 and C_4 into the equilibrium equations (36) and (37) results in

$$D\frac{d^4W_t(y)}{dy^4} + Etk^2W_t(y) = Etk^2h\left(1 - \frac{y^2}{b^2}\right) + Etk\left\{\frac{k}{4b}\int_{-b}^{b}\left[W_t(y) + W_b(y)\right]dy\right\} \tag{44}$$

and

$$D\frac{d^4W_b(y)}{dy^4} + Etk^2W_b(y) = -Etk^2h\left(1 - \frac{y^2}{b^2}\right) + Etk\left\{\frac{k}{4b}\int_{-b}^{b}\left[W_t(y) + W_b(y)\right]dy\right\} \tag{45}$$

The two foregoing equations are identical with the equilibrium equations derived in the preceding section since the integral appearing in these equations is recognized as ϵ_{x_o}, the strain at the surface which passes through the beam edges.

Solution of Basic Equations

The differential equations for the deflections of the covers (eqs. (17) and (18)) are

$$D\frac{d^4W_t(y)}{dy^4} + Etk^2W_t(y) = Etk^2h\left(1 - \frac{y^2}{b^2}\right) + Etk\epsilon_{x_o}$$

and

$$D\frac{d^4W_b(y)}{dy^4} + Etk^2W_b(y) = -Etk^2h\left(1 - \frac{y^2}{b^2}\right) + Etk\epsilon_{x_o}$$

These equations upon division by D become

$$\frac{d^4 w_t(y)}{dy^4} + 4\lambda^4 w_t(y) = 4\lambda^4 h\left(1 - \frac{y^2}{b^2}\right) + 4\lambda^4 \frac{\epsilon_{x_o}}{k} \tag{46}$$

and

$$\frac{d^4 w_b(y)}{dy^4} + 4\lambda^4 w_b(y) = -4\lambda^4 h\left(1 - \frac{y^2}{b^2}\right) + 4\lambda^4 \frac{\epsilon_{x_o}}{k} \tag{47}$$

where

$$4\lambda^4 = \frac{Etk^2}{D}$$

The solutions are

$$w_t(y) = A_t \cosh \lambda y \cos \lambda y + B_t \sinh \lambda y \sin \lambda y + h\left(1 - \frac{y^2}{b^2}\right) + \frac{\epsilon_{x_o}}{k} \tag{48}$$

and

$$w_b(y) = A_b \cosh \lambda y \cos \lambda y + B_b \sinh \lambda y \sin \lambda y - h\left(1 - \frac{y^2}{b^2}\right) + \frac{\epsilon_{x_o}}{k} \tag{49}$$

where only two arbitrary constants are required in each solution because of symmetry.

If use is made of the boundary conditions and the relation for determining ϵ_{x_o}, the constants become

$$\frac{A_t}{h} = -\frac{4}{\gamma}\frac{\sinh\gamma\sin\gamma}{\sinh 2\gamma + \sin 2\gamma} -$$

$$\frac{\mu\frac{t}{h}}{\sqrt{3(1-\mu^2)}}\left[\frac{(\sinh 2\gamma + \sin 2\gamma)\sinh\gamma\sin\gamma - (\sinh 2\gamma - \sin 2\gamma)\cosh\gamma\cos\gamma}{(\sinh 2\gamma + \sin 2\gamma)(\cosh 2\gamma + \cos 2\gamma)}\right] \quad (50)$$

$$\frac{A_b}{h} = \frac{4}{\gamma}\frac{\sinh\gamma\sin\gamma}{\sinh 2\gamma + \sin 2\gamma} -$$

$$\frac{\mu\frac{t}{h}}{\sqrt{3(1-\mu^2)}}\left[\frac{(\sinh 2\gamma + \sin 2\gamma)\sinh\gamma\sin\gamma - (\sinh 2\gamma - \sin 2\gamma)\cosh\gamma\cos\gamma}{(\sinh 2\gamma + \sin 2\gamma)(\cosh 2\gamma + \cos 2\gamma)}\right] \quad (51)$$

$$\frac{B_t}{h} = \frac{4}{\gamma}\frac{\cosh\gamma\cos\gamma}{\sinh 2\gamma + \sin 2\gamma} +$$

$$\frac{\mu\frac{t}{h}}{\sqrt{3(1-\mu^2)}}\left[\frac{(\sinh 2\gamma - \sin 2\gamma)\sinh\gamma\sin\gamma + (\sinh 2\gamma + \sin 2\gamma)\cosh\gamma\cos\gamma}{(\sinh 2\gamma + \sin 2\gamma)(\cosh 2\gamma + \cos 2\gamma)}\right] \quad (52)$$

and

$$\frac{B_b}{h} = -\frac{4}{\gamma}\frac{\cosh\gamma\cos\gamma}{\sinh 2\gamma + \sin 2\gamma} + \frac{\mu\frac{t}{h}}{\sqrt{3(1-\mu^2)}}\left[\frac{(\sinh 2\gamma - \sin 2\gamma)\sinh\gamma\sin\gamma + (\sinh 2\gamma + \sin 2\gamma)\cosh\gamma\cos\gamma}{(\sinh 2\gamma + \sin 2\gamma)(\cosh 2\gamma + \cos 2\gamma)}\right] \quad (53)$$

where

$$\gamma = \lambda b = \sqrt[4]{12(1-\mu^2)}\sqrt{\frac{kr}{t/h}}$$

and

$$b^2 = 2rh$$

The relation for ϵ_{x_o} obtained from equation (20) and used in evaluating the constants A_t, A_b, B_t, and B_b is $\epsilon_{x_o} = -\frac{\mu k^2 b^2}{2\gamma^2}\frac{\sinh 2\gamma - \sin 2\gamma}{\sinh 2\gamma + \sin 2\gamma}$. This result shows that the shift of the neutral surface is in the direction of the tension cover plate.

With the constants defined, the deflection at any point in the cross section can be determined.

Beam Bending Moment

The beam bending moment at any cross section is determined from the sum of the moments acting on the cross section. If the bending moments of the covers about their own middle surfaces and the bending moments of the axial forces N_{x_t} and N_{x_b} about the neutral surface of the cross section are taken into account, the total bending moment is

$$m = \int_{-b}^{b} M_{x_t}\,dy + \int_{-b}^{b} M_{x_b}\,dy - \int_{-b}^{b} N_{x_t}\left[h\left(1 - \frac{y^2}{b^2}\right) + \frac{\epsilon_{x_o}}{k} - W_t(y)\right]dy + \int_{-b}^{b} N_{x_b}\left[h\left(1 - \frac{y^2}{b^2}\right) - \frac{\epsilon_{x_o}}{k} + W_b(y)\right]dy \tag{54}$$

After substitution for N_{x_t} and N_{x_b} as given by the force-strain relationships (11) and (12) and for M_{x_t} and M_{x_b} as given by the following moment-distortion relationships obtained from plate theory,

$$M_{x_t} = -D\left[-k + \mu \frac{d^2W_t(y)}{dy^2}\right] \tag{55}$$

and

$$M_{x_b} = -D\left[-k + \mu \frac{d^2W_b(y)}{dy^2}\right] \tag{56}$$

equation (54) becomes

$$m = -D\int_{-b}^{b}\left\{-2k + \mu\left[\frac{d^2W_t(y)}{dy^2} + \frac{d^2W_b(y)}{dy^2}\right]\right\}dy +$$

$$Etk\int_{-b}^{b}\left[h\left(1 - \frac{y^2}{b^2}\right) + \frac{\epsilon_{x_o}}{k} - W_t(y)\right]^2 dy +$$

$$Etk\int_{-b}^{b}\left[h\left(1 - \frac{y^2}{b^2}\right) - \frac{\epsilon_{x_o}}{k} + W_b(y)\right]^2 dy \qquad (57)$$

With the bending moment reduced to a function of the deflections and the deflections defined by the equations of the preceding section, the bending moment can be evaluated to give in terms of nondimensional parameters

$$\frac{mr/EI_o}{t/h} = \frac{kr}{t/h}\left\{\frac{5}{32(1-\mu^2)}\left(\frac{t}{h}\right)^2 + \right.$$

$$\frac{15(\cosh 2\gamma + \cos 2\gamma)}{16\gamma^3(\sinh 2\gamma + \sin 2\gamma)}\left[1 - \frac{\mu^2}{8(1-\mu^2)}\left(\frac{t}{h}\right)^2\frac{\gamma^2(\cosh 2\gamma - \cos 2\gamma)}{(\cosh 2\gamma + \cos 2\gamma)}\right] -$$

$$\left.\frac{15(\cosh 2\gamma \cos 2\gamma + 1)}{4\gamma^2(\sinh 2\gamma + \sin 2\gamma)^2}\left[1 + \frac{\mu^2}{24(1-\mu^2)}\left(\frac{t}{h}\right)^2\frac{\gamma^2\sinh 2\gamma \sin 2\gamma}{(\cosh 2\gamma \cos 2\gamma + 1)}\right]\right\} \qquad (58)$$

where

$$\frac{kr}{t/h} = \frac{\gamma^2}{2\sqrt{3(1-\mu^2)}}$$

and I_0, the moment of inertia of the undeformed cross section, in which the moment of inertia of the plates about their own middle surfaces is neglected is defined as

$$I_0 = 2\int_{-b}^{b}\left[h\left(1 - \frac{y^2}{b^2}\right)\right]^2 t\,dy = \frac{32}{15}tbh^2$$

The moment parameter $\frac{mr/EI_0}{t/h}$, plotted against the beam-curvature parameter $\frac{kr}{t/h}$ for several values of t/h, is shown in figure 2.

Cross-Section Distortion

The magnitude of the cross-section deformation may be given in terms of the ratio of beam depth under loading to beam depth of the unloaded section measured at the center of the cross section. That is,

$$\frac{h_t(0) + h_b(0)}{2h} = \frac{4\sinh\gamma\sin\gamma}{\gamma(\sinh 2\gamma + \sin 2\gamma)} \tag{59}$$

where

$$h_t(y) = h\left(1 - \frac{y^2}{b^2}\right) - W_t(y)$$

and

$$h_b(y) = h\left(1 - \frac{y^2}{b^2}\right) + W_b(y)$$

This ratio, plotted against the beam-curvature parameter, is shown in figure 3.

The shape of the deformed cross section may be found from the equations for chordwise deflection of the covers. If the small effect of ϵ_{x_o}

is neglected so that $W_t(y) = -W_b(y)$, the deformed shape of each cover is given by

$$\frac{h_t(y)}{h} = \frac{h_b(y)}{h} = \frac{4(\sinh \gamma \sin \gamma \cosh \lambda y \cos \lambda y - \cosh \gamma \cos \gamma \sinh \lambda y \sin \lambda y)}{\gamma(\sinh 2\gamma + \sin 2\gamma)} \tag{60}$$

This ratio is illustrated in figure 4 for a loading of $m = 0.285 \frac{EtI_0}{rh}$.

Axial Stress

From a preceding section (eqs. (11) to (14)), the nondimensional axial-stress ratios can be written

$$\frac{N_{x_t}}{Etkh} = -\left[1 - \frac{y^2}{b^2} + \frac{\epsilon_{x_o}}{kh} - \frac{W_t(y)}{h}\right] \tag{61}$$

and

$$\frac{N_{x_b}}{Etkh} = \left[1 - \frac{y^2}{b^2} - \frac{\epsilon_{x_o}}{kh} + \frac{W_b(y)}{h}\right] \tag{62}$$

In general, the nondimensional axial-stress ratios at the greatest distance from the neutral surface are of primary interest. At $y = 0$, therefore,

$$\frac{\left(N_{x_t}\right)_{y=0}}{Etkh} = -\left\{\frac{4 \sinh \gamma \sin \gamma}{\gamma(\sinh 2\gamma + \sin 2\gamma)}\left[1 + \frac{\mu}{4\sqrt{3(1-\mu^2)}} \frac{t}{h} \gamma(\coth \gamma - \cot \gamma)\right]\right\} \tag{63}$$

and

$$\frac{\left(N_{x_b}\right)_{y=0}}{Etkh} = \left\{\frac{4 \sinh \gamma \sin \gamma}{\gamma(\sinh 2\gamma + \sin 2\gamma)}\left[1 - \frac{\mu}{4\sqrt{3(1-\mu^2)}} \frac{t}{h} \gamma(\coth \gamma - \cot \gamma)\right]\right\} \tag{64}$$

The preceding equations are illustrated in figure 5 in terms of $\frac{-\left(N_{x_t}\right)_{y=0}}{Etkh}$ and $\frac{\left(N_{x_b}\right)_{y=0}}{Etkh}$ plotted against the beam-curvature parameter $\frac{kr}{t/h}$ for several values of t/h.

The curves plotted in figure 5 can be presented in another form by referring the stress ratios to the elementary-beam-theory stress at equivalent moment rather than at equivalent curvature. Thus,

$$\frac{-\left(N_{x_t}\right)_{y=0}}{tmh/I_0} = \frac{\frac{-\left(N_{x_t}\right)_{y=0}}{Etkh}\frac{kr}{t/h}}{\frac{mr/EI_0}{t/h}}$$

and

$$\frac{\left(N_{x_b}\right)_{y=0}}{tmh/I_0} = \frac{\frac{\left(N_{x_b}\right)_{y=0}}{Etkh}\frac{kr}{t/h}}{\frac{mr/EI_0}{t/h}}$$

In figure 6, these nondimensional stress ratios are plotted against the nondimensional moment parameter, with the small effect of changes in the t/h ratio being neglected.

Approximate Formulas

When the shift in the neutral surface is neglected, simplified expressions for deflection, bending moment, and axial stress are obtainable from the resulting equations by expanding functions of γ into finite

power series to give

$$\frac{W_t(y)}{h} = -\frac{W_b(y)}{h}$$

$$= -\frac{1 - \frac{\gamma^4}{90}}{1 + \frac{2\gamma^4}{15}} \cosh \lambda y \cos \lambda y + \frac{1}{\gamma^2} \frac{1 - \frac{\gamma^4}{6}}{1 + \frac{2\gamma^4}{15}} \sinh \lambda y \sin \lambda y + 1 - \frac{y^2}{b^2} \tag{65}$$

$$\frac{mr/EI_0}{t/h} = \frac{kr}{t/h} \frac{1}{\left(1 + \frac{2\gamma^4}{15}\right)^2} \tag{66}$$

and

$$\frac{N_{x_t}}{Etkh} = \frac{-N_{x_b}}{Etkh}$$

$$= -\frac{1 - \frac{\gamma^4}{90}}{1 + \frac{2\gamma^4}{15}} \cosh \lambda y \cos \lambda y + \frac{1}{\gamma^2} \frac{1 - \frac{\gamma^4}{6}}{1 + \frac{2\gamma^4}{15}} \sinh \lambda y \sin \lambda y \tag{67}$$

The foregoing approximate formulas are considered to be very satisfactory in the region $0 \leqq \frac{kr}{t/h} \leqq 0.6$. The maximum errors to be expected are of the order of several percent.

REFERENCES

1. Brazier, L. G.: The Flexure of Thin Cylindrical Shells and Other "Thin" Sections. R. & M. No. 1081, British A.R.C., 1926.

2. Batdorf, S. B., Schildcrout, Murry, and Stein, Manuel: Critical Combinations of Shear and Longitudinal Direct Stress for Long Plates With Transverse Curvature. NACA TN 1347, 1947.

3. Timoshenko, S.: Theory of Elastic Stability. McGraw-Hill Book Co., Inc., 1936, p. 465.

4. Marguerre, K.: Zur Theorie der gekrümmten Platte grosser Formänderung. Proc. Fifth Int. Cong. Appl. Mech. (Cambridge, Mass., 1938), John Wiley & Sons, Inc., 1939, pp. 93-101.

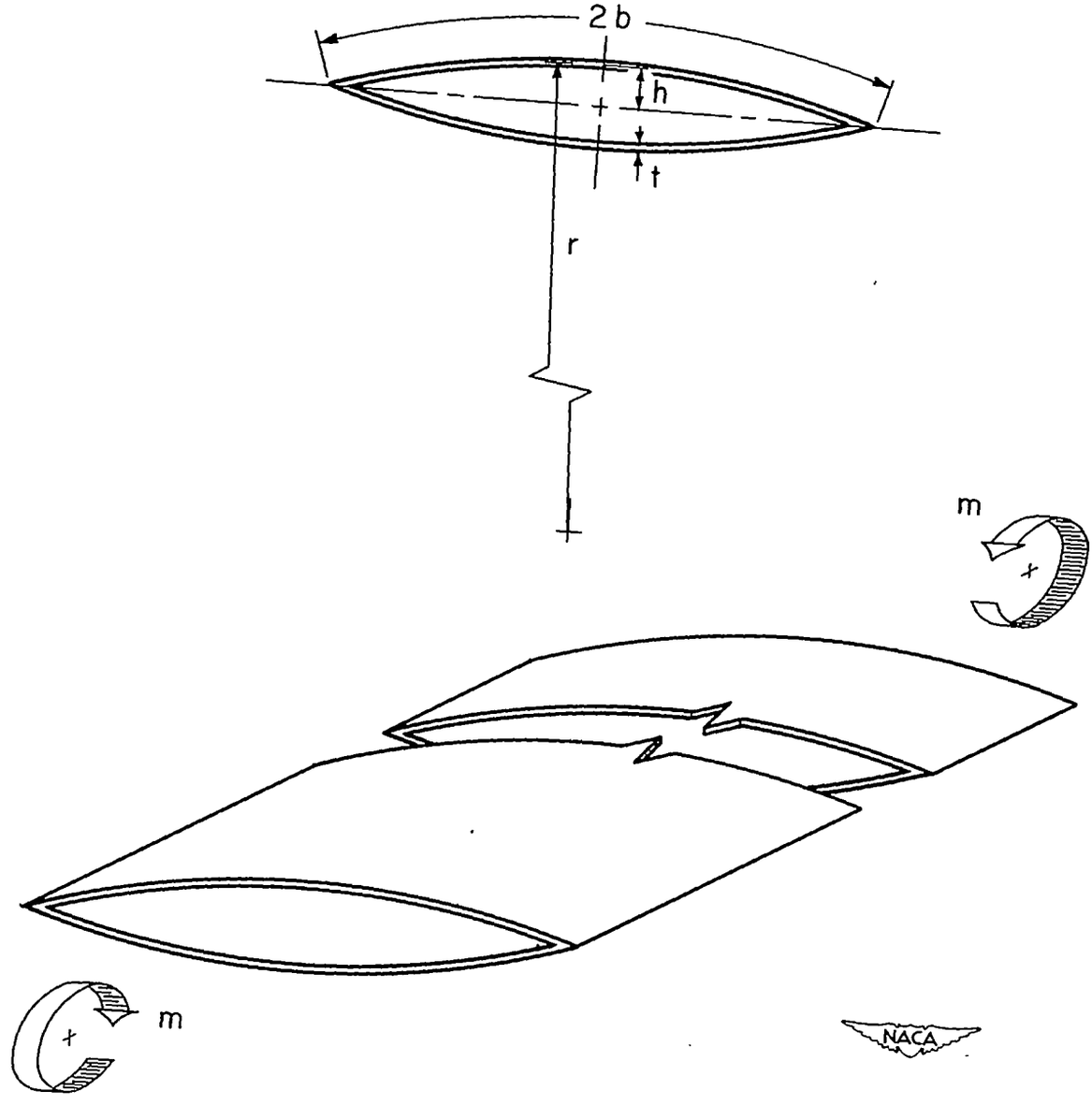

Figure 1.- A thin, infinitely long, doubly symmetric, circular-arc cross-section beam under a loading of pure bending moment.

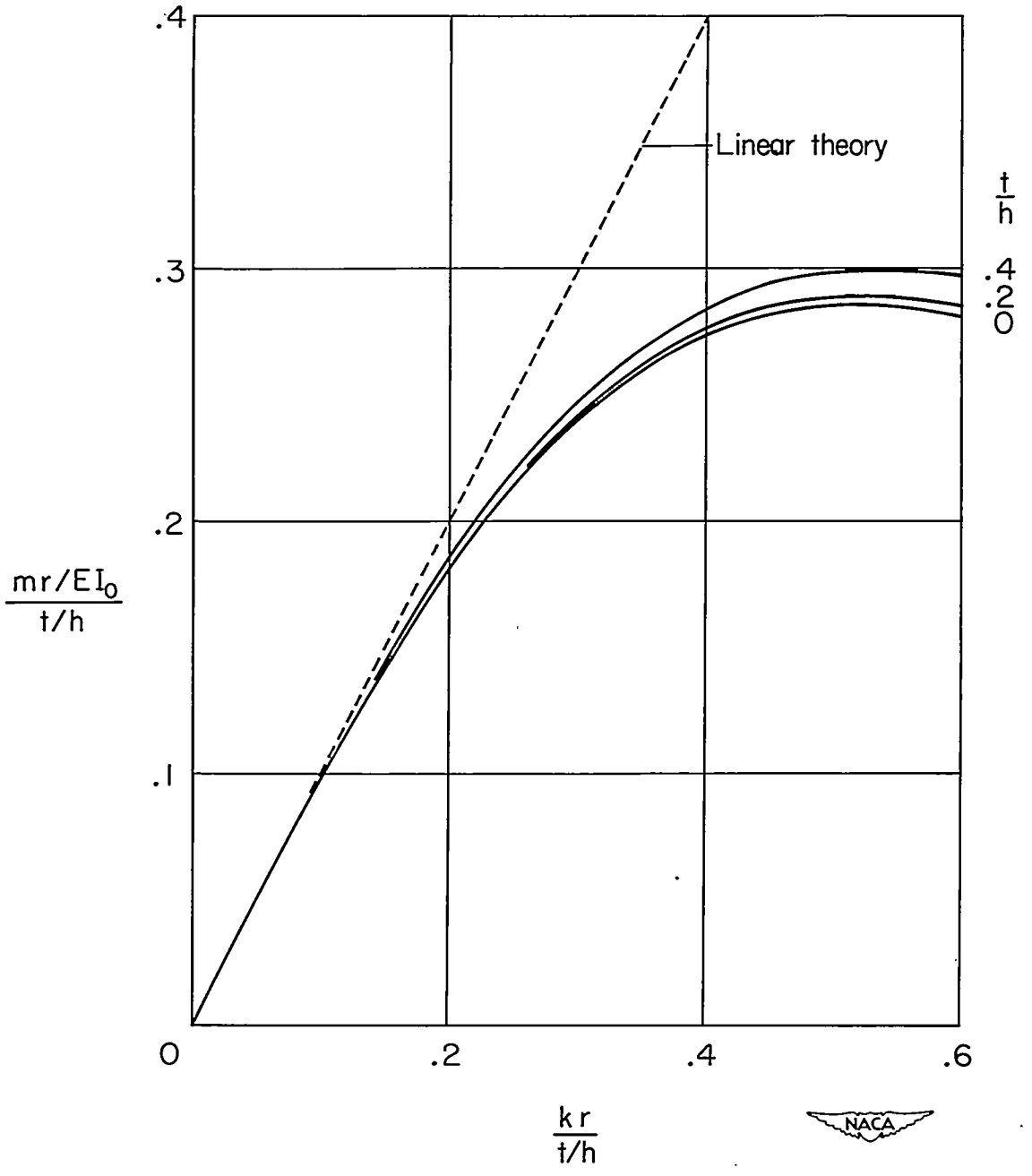

Figure 2.- Relationship between bending moment and longitudinal beam curvature. $\left(I_0 = \frac{32}{15} tbh^2 = \frac{8}{15} \frac{tb^5}{r^2}\right)$

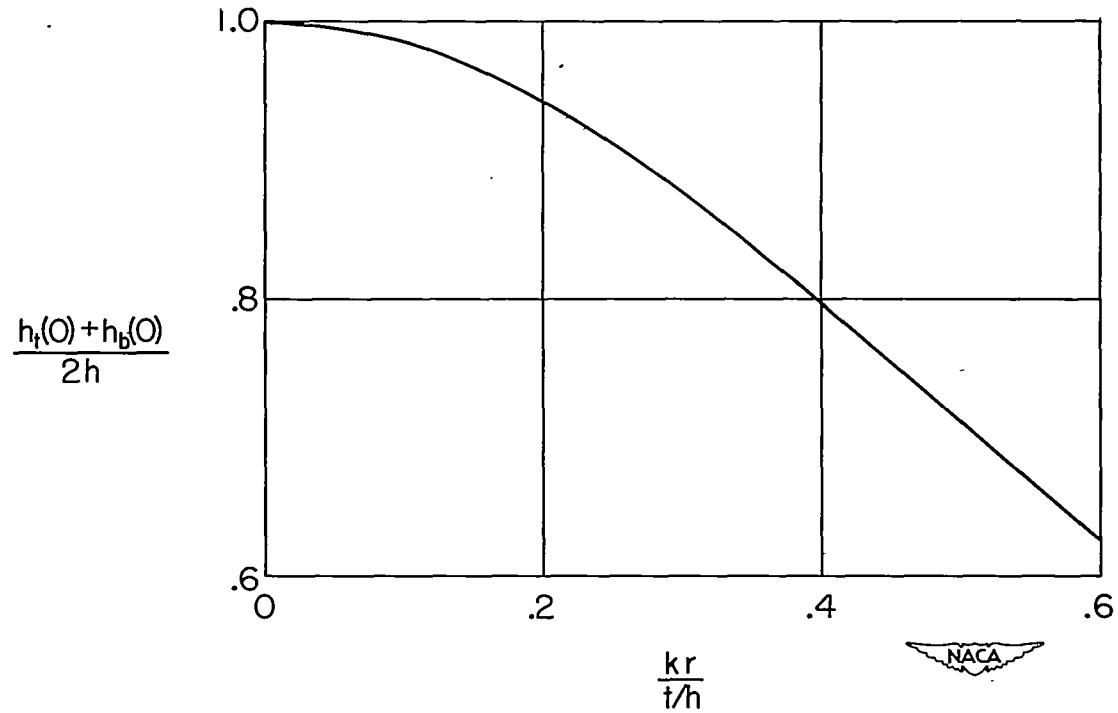

Figure 3.- Ratio of beam thickness of loaded section to beam thickness of unloaded section.

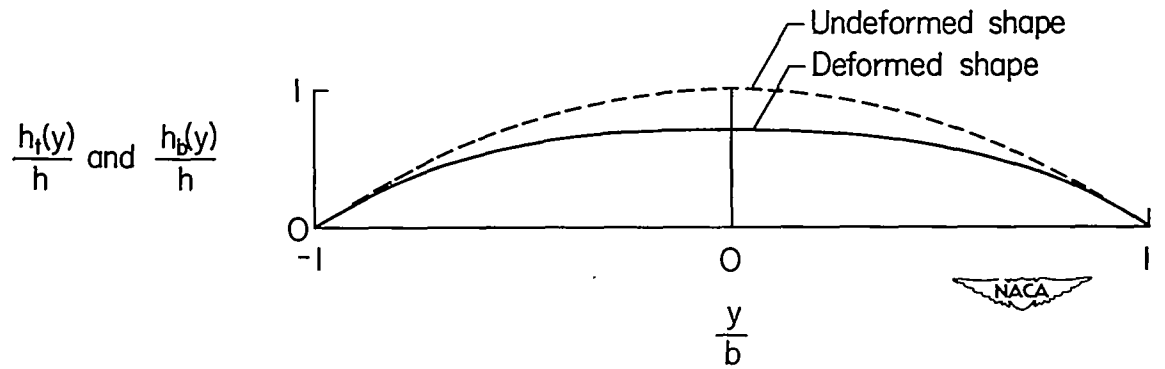

Figure 4.- Chordwise cover deflections under a loading of $m = 0.285 \frac{EtI_0}{rh}$. Neutral-surface shift is neglected.

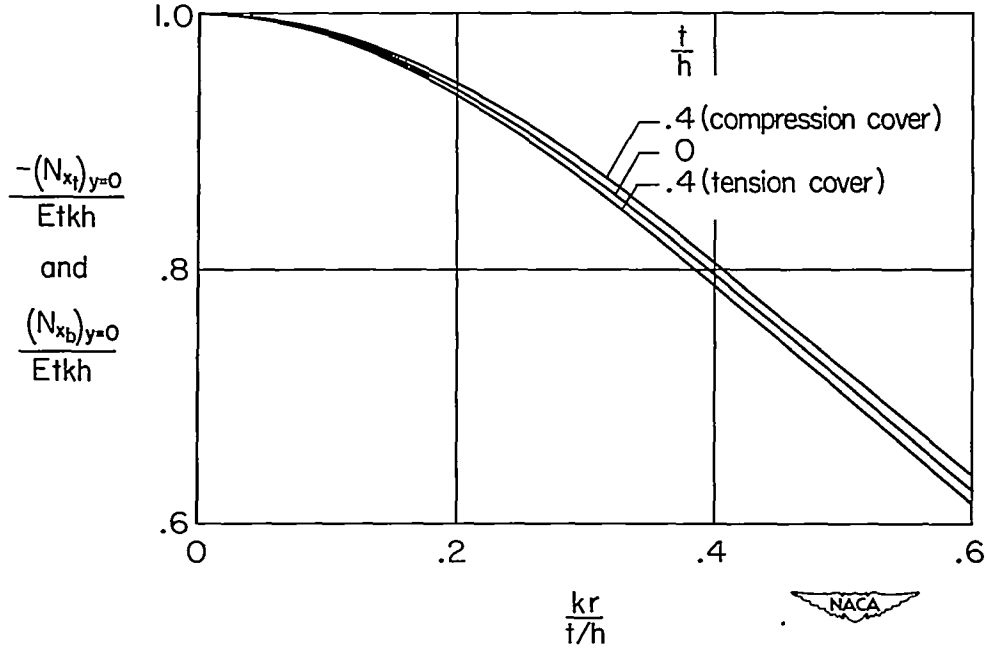

Figure 5.- Ratio of midchord axial stress to elementary-beam-theory stress Ekh at equivalent curvature.

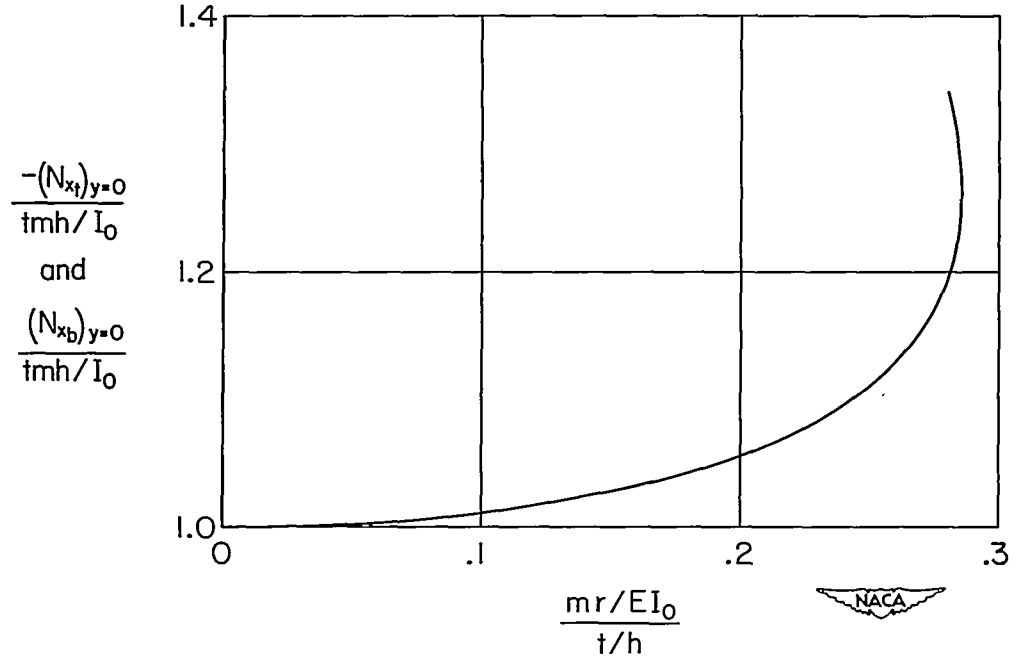

Figure 6.- Ratio of midchord axial stress to elementary-beam-theory stress mh/I_0 at equivalent moment. Neutral-surface shift is neglected.

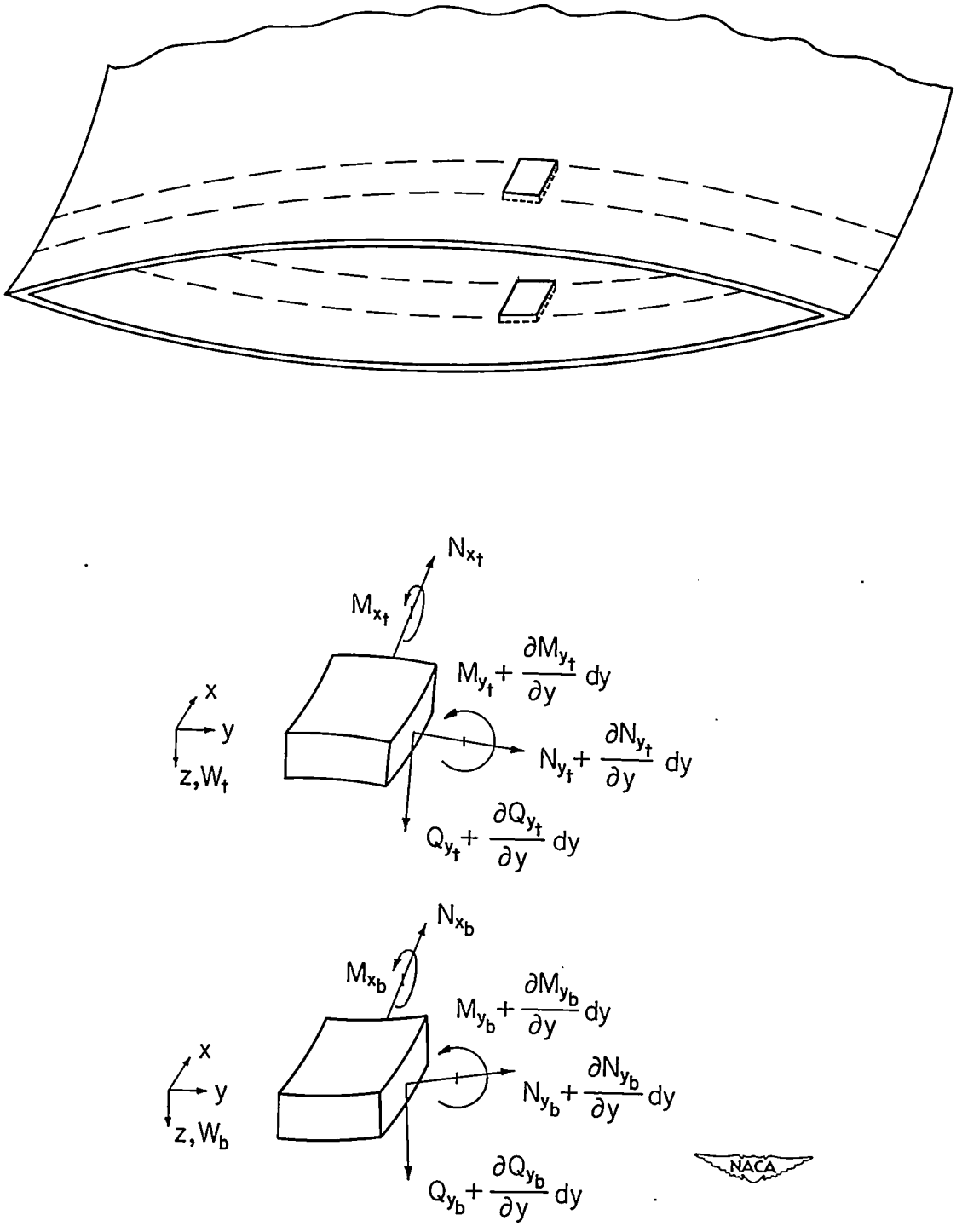

Figure 7.- Forces and moments acting on cover elements.